Research paper

Cite as: Gumowska M, Dobruch-Sobczak K: Differentiation of triple-negative breast cancer and benign breast lesions using multiparametric ultrasonography. J Ultrason 2025; 25: 23. doi: 10.15557/JoU.2025.0023.

Submitted: 14.04.2025
Accepted: 15.07.2025
Published: 30.09.2025

Differentiation of triple-negative breast cancer and benign breast lesions using multiparametric ultrasonography

Magdalena Gumowska, Katarzyna Sylwia Dobruch-Sobczak

Second Radiology Department, Maria Skłodowska-Curie Memorial Cancer Center and Institute of Oncology, Warsaw, Poland

Corresponding author: Magdalena Gumowska; e-mail: m.ewabielawska@gmail.com

DOI: 10.15557/JoU.2025.0023

Keywords
ultrasound; sonoelastography; TNBC

Abstract

Aim: Assessment of features of triple-negative breast cancer (TNBC) and benign breast lesions in multiparametric ultrasonography, with an emphasis on the added value of sonoelastography. **Material and methods:** Forty-one women with TNBC and 51 with benign breast lesions, underwent sonographic evaluation at the Maria Skłodowska-Curie National Research Institute of Oncology, Warsaw, between 05.2020 and 11.2023. A retrospective analysis was conducted. The following features of the tumors were evaluated: B-mode characteristics, presence of vascularity, and tissue stiffness in shear wave elastography. Two sets of data were extracted from the database: the first encompassing the total group of tumors (TG), the second comprising small lesions (<20 mm, SG). Statistical analysis for both groups was run independently to investigate if and how the size of the tumor would influence the diagnostic accuracy of the sonographic evaluation. TNBCs and benign entities were compared with t-Student's test, Mann-Whitney U test, Pearson's chi-square test or Fisher's exact test. ROC analysis and logistic regression were conducted. **Results:** For TG, ultrasound showed high predictive accuracy (AUC >0.8) for the following single parameters: elastography other than soft (>80 kPa) and irregular shape. Adding 2 features improved performance, with the highest AUC (0.858) for non-circumscribed margins and irregular shape. For SG, single parameters with the best predictive effectiveness (AUC >0,8) were: irregular shape, elastography other than soft (>80 kPa), and noncircumscribed margins. Elastography other than soft revealed high specificity. Combinations of features with AUC >0.9 were: irregular shape and hypoechogenicity; non-circumscribed margins and hypoechogenicity; and non-circumscribed margins, irregular shape, and hypoechogenicity. **Conclusions:** Accurate assessment of shape and margins, enhanced by information about tissue stiffness, substantially improves differentiation between TNBC and benign breast lesions.

Introduction

The term triple-negative breast cancer (TNBC) encompasses a heterogeneous group of tumors that express neither estrogen nor progesterone receptors and lack overexpression of human epidermal growth factor receptor 2 (HER2).

Diagnosis of TNBC accounts for approximately 10–15% of breast cancer cases (BC) and carries an unfavorable prognosis. It occurs more often than other subtypes in younger populations, especially in carriers of *BRCA* and *PALB2* mutations, and during pregnancy and lactation[1–3]. A meta-analysis conducted by Li *et al.*[4] showed that women using oral contraceptives are more likely to develop TNBC compared to the general population, especially when additional risk factors coexist. Compared with other subtypes, TNBC is more often diagnosed at a more advanced stage, and patients are at increased risk of early distant metastases and recurrence.

Radiologic evaluation is challenging due to the heterogeneity of the tumors and because radiological features of TNBC and benign tumors, such as fibroadenoma (FA), may overlap. According to the literature, despite its aggressive nature, up to 41% of TNBCs exhibit benign morphology on radiological assessment[2,5–7].

Mammography commonly shows an oval/round tumor of high density with partially circumscribed margins. It may lack typical malignant features[2].

MRI is known to provide the highest detection rates, but is not free from diagnostic dilemmas, especially in cases with enhancing internal septa, which may be misinterpreted as the internal septa observed in FA – or with high intratumoral T2-weighted signal intensity, which is also seen in cystic lesions[2,8].

The sonographic appearance of TNBC shows a spectrum of features encountered in both benign and malignant lesions. In a study by Zhang *et al.*, two patterns of TNBC appearance were described. The first group was characterized by irregular shape, lobular margins, absence of microcalcification, and hypovascularity; the second group had an oval shape, hypovascularity, and microlobular margins[9].

Small cancers are particularly problematic, as they may resemble FA or complicated cysts. A study by Yoon *et al.*[1] showed that among TNBCs measuring <2 cm, 7% were assigned to the BI-RADS3 and 27% to the BI-RADS4a category.

The study aimed to identify differences between TNBC and FA-like lesions using multiparametric ultrasonography.

Materials and methods

A retrospective analysis of data collected between 05.2020 and 11.2023 was conducted. A total of 92 patients with 92 lesions underwent sonographic evaluation in the Second Radiology Department of the Maria Skłodowska-Curie Memorial Cancer Center and Institute of Oncology, Warsaw, Poland. TNBCs were diagnosed in 41 women, and a diagnosis of benign lesion (FA group) was established in 51 women. The inclusion criteria were as follows: solitary TNBC confirmed by core needle biopsy (CNB) before treatment, solitary lesion, most commonly FA, confirmed by CNB or assessed as BI-RADS3 category, downgraded after two years of observation to BI-RADS2. Exclusion criteria were: patients undergoing neoadjuvant chemotherapy (NAC), recurrence after treatment, and patients with multiple lesions.

First, features of the total group (TG) of tumors assessed during the sonographic examination were compared. Then, a group of tumors smaller than 20 mm was extracted (small group, SG) to investigate whether – and how – lesion size would affect differentiation capabilities.

Histology

All TNBCs were confirmed by CNB. FA-like lesions were confirmed either by CNB or based on two years of stability on follow-up. CNBs were performed using a 14G needle, retrieving 3 to 5 tissue cores from each lesion. A pathologist with 28 years of experience in breast oncology assessed the specimens.

Data acquisition

Examinations were performed by four radiologists (10–25 years of experience in breast sonography, >2 years of experience in sonoelastography), using an ultrasound scanner (Aixplorer System, SuperSonic Imagine) with a linear L18–5 MHz transducer equipped with shear wave elastography (SWE).

Two perpendicular cross-sections were obtained. B-mode features of the lesions were evaluated according to the ACR BI-RADS 2013 Atlas and included: shape, orientation, margin, echo pattern, posterior features, presence of calcifications, and skin changes.

Tumor vascularity was assessed using Color Doppler and AngioPlus modes with low wall filter settings (2–3 cm/s) to pick up slow velocity signals. Vascularity in both modes was compared to identify additional small vessels in the AngioPlus mode, which are considered a sign of neovascularity.

The stiffness of the tumor and surrounding tissue was evaluated using SWE, according to the guidelines of the World Federation of Societies for Ultrasound in Medicine and Biology[10]. A cut-off value for maximal elasticity (E_{max}) <80 kPa was determined for soft lesions, 80–160 kPa for intermediate stiffness, and E_{max} >160 kPa for hard tissue. One cross-section through the lesion was obtained. Elasticity was measured within a 2 mm ROI placed in the hardest part of the lesion or up to 2 mm from the lesion's margin.

Statistical methods

Analysis was performed using R: A Language and Environment for Statistical Computing, version 4.1.2. Depending on the distribution, numerical variables were described using mean ± SD or median (IQR). Normality was assessed with the Shapiro-Wilk test and verified using skewness and kurtosis. Variance homogeneity was assessed with Levene's test. TNBCs and FAs were compared with the Student's *t*-test, Mann-Whitney *U* test, Pearson's chi-square test, or Fisher's exact test, as appropriate. Receiver operating characteristic (ROC) analysis was performed to evaluate the predictive value of the analyzed variables and their combinations. The optimal cut-off was calculated with the Youden method. Statistical tests assumed significance when the *p*-value was lower than 0.05.

Ethical approval

The study was approved by the ethics committee of the Maria Skłodowska-Curie Memorial Cancer Center and Institute of Oncology (no 49/2018, 27 September 2018). As it was a retrospective study, no written informed consent was obtained.

Results

Calculations were performed separately for the total group (TG) and for lesions <20 mm (SG). Detailed results are available in the Supplementary material (Tab. S1, Tab. S2, Tab. S3, Fig. S1, Fig. S2, Tab. S4, Tab. S5).

First, individual features were assessed. For TG, the mean age in the TNBC group was 10 years higher than in the FA group (55 vs. 45 years, respectively, $p = 0.001$). The size of TNBCs was 12 mm larger than that of FAs ($p < 0.001$). Irregular shape was significantly more common in TNBCs (95.1%) compared to FAs (31.4%), while oval/round shape was less common in the TNBC group (4.9%, $n = 2$) compared to the FA group (68.6%), ($p < 0.001$).

Type of margins significantly differentiated the groups ($p < 0.001$). All TNBCs were characterized by non-circumscribed margins, while in FAs it was observed in only 41.2% of cases. Vascularity was present in nearly all TNBCs (92.7%) and in 62.7% of FAs ($p = 0.002$). A significant difference between TNBCs and FAs was also observed in tissue stiffness ($p < 0.001$): the soft category was less common in TNBCs than in FAs (22.0% vs 88.2%), while the hard category was observed only in TNBCs (51.2%). Skin thickening (>2 mm) occurred in 22.0% of TNBCs and was not present in any FAs ($p < 0.001$).

For SG, the results were similar; additionally, a significant difference was noted for echogenicity – 93.8% of TNBCs were hypoechogenic, compared to 36.6% of FAs ($p < 0.001$) (Tab. 1).

Tab. 1. Characteristics and comparison of TNBC and FA in TG and SG

Variable	Total group, TG (*n* = 92)				SG, size ≤20 mm (*n* = 57)			
	TNBC (*n* = 41, 44.6%)	**FA (*n* = 51, 55.4%)**	**MD (95% CI)**	***p***	**TNBC (*n* = 16, 28.1%)**	**FA (*n* = 41, 71.9%)**	**MD (95% CI)**	***p***
Age, years	55.22 ± 11.76	45.57 ± 15.45	9.65 (3.85;15.46)	**0.001**[1]	55.75 ± 9.53	47.44 ± 14.60	8.31 (0.39;16.23)	**0.040**[1]
Size, mm	26.00 (16.00;43.00)	14.00 (11.50;18.00)	12.00 (5.00;18.00)	**<0.001**[2]	13.44 ± 3.63	13.10 ± 3.69	0.34 (−1.83;2.51)	0.755[1]
Size								
≤20 mm	16 (39.0)	41 (80.4)	–	**<0.001**	0 (0.0)	0 (0.0)	–	–
>20 mm	25 (61.0)	10 (19.6)			16 (100.0)	41 (100.0)		
Shape								
Oval/round	2 (4.9)	35 (68.6)	–	**<0.001**	1 (6.2)	31 (75.6)	–	**<0.001**
Irregular	39 (95.1)	16 (31.4)			15 (93.8)	10 (24.4)		
Orientation								
Parallel	39 (95.1)	51 (100.0)	–	0.196	15 (93.8)	41 (100.0)	–	0.281[3]
Non-parallel	2 (4.9)	0 (0.0)			1 (6.2)	0 (0.0)		
Margins								
Circumscribed	0 (0.0)	30 (58.8)	–	**<0.001**	0 (0.0)	25 (61.0)	–	**<0.001**
Non-circumscribed	41 (100.0)	21 (41.2)			16 (100.0)	16 (39.0)		
Non-circumscribed margins by type*								
Angular/spicular	19 (46.3)	1 (5.6)	–	**0.006**	6 (37.5)	1 (7.1)	–	0.172[3]
Macro/microlobular	5 (12.2)	6 (33.3)			2 (12.5)	2 (14.3)		
Indistinct	17 (41.5)	11 (61.1)			8 (50.0)	11 (78.6)		
Echogenicity								
Hypoechoic	22 (53.7)	16 (31.4)	–	0.052	15 (93.8)	15 (36.6)	–	**<0.001**
Other than hypoechoic	19 (46.3)	35 (68.6)			1 (6.2)	26 (63.4)		
Posterior features								
Yes	34 (82.9)	34 (66.7)	–	0.127	10 (62.5)	27 (65.9)	–	>0.999
No	7 (17.1)	17 (33.3)			6 (37.5)	14 (34.1)		
Skin								
Normal	32 (78.0)	51 (100.0)	–	**<0.001**[3]	16 (100.0)	41 (100.0)	–	**–**
>2 mm	9 (22.0)	0 (0.0)			0 (0.0)	0 (0.0)		
Hyperechogenic halo								
Yes	28 (68.3)	8 (15.7)	–	**<0.001**	9 (56.2)	7 (17.1)	–	**0.007**[3]
No	13 (31.7)	43 (84.3)			7 (43.8)	34 (82.9)		
Vascularity in CD								
Yes	38 (92.7)	32 (62.7)	–	**0.002**	14 (87.5)	23 (56.1)	–	0.054
No	3 (7.3)	19 (37.3)			2 (12.5)	18 (43.9)		
AngioPlus compared to CD**								
Even	20 (64.5)	41 (87.2)	–	**0.036**	8 (72.7)	33 (89.2)	–	0.327[3]
AngioPlus dominance	11 (35.5)	6 (12.8)			3 (27.3)	4 (10.8)		
Elastography								
Soft <80 kPa	9 (22.0)	45 (88.2)	–	**<0.001**	5 (31.2)	38 (92.7)	–	**<0.001**[3]
Intermediate T3, 80–160 kPa	11 (26.8)	6 (11.8)			6 (37.5)	3 (7.3)		
Hard >160 kPa	21 (51.2)	0 (0.0)			5 (31.2)	0 (0.0)		
Calcification								
Yes	10 (25.6)	13 (25.5)	–	>0.999	2 (12.5)	11 (26.8)	–	0.313[3]
No	29 (74.4)	38 (74.5)			14 (87.5)	30 (73.2)		

Numerical parameters were described with mean ± standard deviation or median (interquartile range), depending on normality. MD – mean/median difference (TNBC vs FA); CI – confidence interval. Groups compared with t–Student test1, Mann–Whitney U test2, Pearson Chi–square test or Fisher's exact test3, as appropriate.
* Proportions vs all observations with irregular margins.
** Proportions vs all observations with available data on AngioPlus (TNBC: *n* = 31, FA: *n* = 47).

Secondly, ROC analysis was performed to determine the effectiveness of individual features in predicting TNBC from FA. Statistically significant results with AUC >0.5 are presented in Tab. 2.

In TG, the highest predictive effectiveness, with AUC >0.8, was noted for elastography values other than soft (>80 kPa) and for irregular shape. The features with AUC values indicating moderate effectiveness in predicting TNBC (AUC from 0.7 to 0.8) included, among others, non-circumscribed margins, presence of a halo, hard category in elastography, and angular/spiculated margins (Tab. 2).

Further ROC analysis was conducted for combinations of features. Combinations that satisfied the following criteria were selected: the outcome of ROC analysis was statistically significant (p <0.05), AUC >0.5, and the AUC of the combination was higher than that of the two features considered separately. Next, combinations of two features were selected as a basis to build three-feature combinations to determine whether it could enhance the recognition of TNBC. The highest outcome was observed for the combination of non-circumscribed margins and irregular shape (AUC = 0.858). Other highly effective combinations were non-circumscribed margins, vascularity in CD, and posterior features (AUC = 0.844), and elastography values other than soft (>80 kPa) combined with irregular shape (AUC = 0.836).

In SG, the highest predictive effectiveness of single features was noted for irregular shape, elastography other than soft (>80 kPa), and non-circumscribed margins (AUC = 0.847, 0.807 and 0.805). Elastography other than soft (>80 kPa) was also found to have high specificity in predicting benign lesions.

The most effective combinations of features for predicting TNBC (AUC >0.9) were: irregular shape and hypoechogenicity; non-circumscribed margins and hypoechogenicity; and non-circumscribed margins and irregular shape and hypoechogenicity.

High predictive quality (AUC >0.8) was also observed for the combination of elastography other than soft (>80 kPa) and hypoechogenicity. Complete statistical data are available in the Supplementary material.

Discussion

The present study demonstrated that differentiation between TNBCs and benign lesions using multiparametric ultrasonography is characterized by high diagnostic accuracy.

In both groups (TG and SG), the most diagnostically valuable individual parameters were similar. In TG, these included elastography other than soft (>80 kPa), irregular shape, and non-circumscribed margins. In SG, key features were irregular shape, elastography other than soft (>80 kPa), non-circumscribed margins, and hypoechogenicity.

The presence of circumscribed margins in TNBCs, often described in literature, is explained by the unique biology of this tumor. The dynamic increase in tumor volume leads to compression of the surrounding tissues, with accompanying inflammatory reaction and a sparse reaction of the glandular stroma[11], which manifests itself in radiological examinations as well-demarcated edges (so-called 'pushing borders')[6,12,13]. Signs of desmoplasia, such as spiculations, hyperechoic halo, and angles[2], are less pronounced compared to luminal subtypes of breast cancer.

Yeo *et al.*[14], in a study comparing small (<2 cm), oval/round TNBCs and FAs (63 vs. 68 observations), found that the degree of morphological abnormalities in TNBC increases with tumor growth, and that differentiation is particularly challenging in small lesions. Aslan *et al.*[15] showed that menopausal status also has a significant effect on TNBC morphology. In the premenopausal group, 55% of TNBC tumors were round or oval in shape, whereas an irregular shape was

Tab. 2. ROC analysis for predicting TNBC type of tumor (vs FA) in TG (p <0.05)

Variable	Cut off**	AUC (95% CI)	Sensitivity	Specificity	Accuracy	PPV	NPV	*p*
Elastography other than soft (>80 kPa)	–	0.831 (0.753; 0.910)	0.78	0.88	0.84	0.84	0.83	**<0.001**
Irregular shape	–	0.819 (0.746; 0.891)	0.95	0.69	0.80	0.71	0.95	**<0.001**
Non-circumscribed margins	–	0.794 (0.726; 0.862)	1.00	0.59	0.77	0.66	1.00	**<0.001**
Halo present	–	0.763 (0.675; 0.851)	0.68	0.84	0.77	0.78	0.77	**<0.001**
Elastography hard (>160 kPa)	–	0.756 (0.679; 0.834)	0.51	1.00	0.78	1.00	0.72	**<0.001**
Size, mm	21.5	0.747 (0.641; 0.853)	0.59	0.84	0.73	0.75	0.72	**<0.001**
Angular/spicular margins	–	0.722 (0.642; 0.802)	0.46	0.98	0.75	0.95	0.69	**<0.001**
Age, years	46.5	0.706 (0.598; 0.814)	0.78	0.61	0.68	0.62	0.77	**0.001**
Vascularity in CD present	–	0.650 (0.571; 0.728)	0.93	0.37	0.62	0.54	0.86	**<0.001**
AngioPlus dominance	–	0.614 (0.515; 0.712)	0.35	0.87	0.67	0.65	0.67	**0.018**
Hypoechogenicity	–	0.611 (0.511; 0.712)	0.54	0.69	0.62	0.58	0.65	**0.031**
Skin >2 mm	–	0.610 (0.546; 0.674)	0.22	1.00	0.65	1.00	0.61	**<0.001**
Non-circumscribed margins other than indistinct *	–	0.599 (0.504; 0.695)	0.41	0.78	0.62	0.61	0.62	**0.039**

AUC – area under curve; CI – confidence interval; PPV – positive predictive value; NPV – negative predictive value
* Non-circumscribed margins other than indistinct encompass: irregular, angular/spicular, and micro/macrolobular margins.
** Cut-off given for numerical variables only.

found in 82.0% of tumors in the postmenopausal group (p <0.001). Candelaria *et al.*[16] demonstrated that the presence of luminal androgen receptor (AR) in the tumor also affects its morphology. AR(+) TNBCs were more likely than AR(−) TNBCs to present calcifications (p = 0.02) and an irregular shape on both MMG (p = 0.05) and US (p = 0.03).

In the present study, all TNBCs exhibited a disturbed margin line, which excluded them from the BI-RADS3 category, although the number of TNBCs <20 mm was limited (16 cases) (Fig. 1).

In addition to margin characteristics, another differentiating feature in the study group was stiffness on SWE. In TG, 51% of TNBCs were characterized by high stiffness (Fig. 2). The parameters "elastography other than soft >80 kPa" and "elastography hard >160 kPa" showed high specificity – E_{max} >160 kPa correlated with the malignant nature of the lesion, indicating a low probability of benign pathology. None of the FA lesions showed high stiffness (Fig. 3). In SG, 30% of TNBCs (5/16 lesions) were classified as soft and almost 70% showed elevated stiffness.

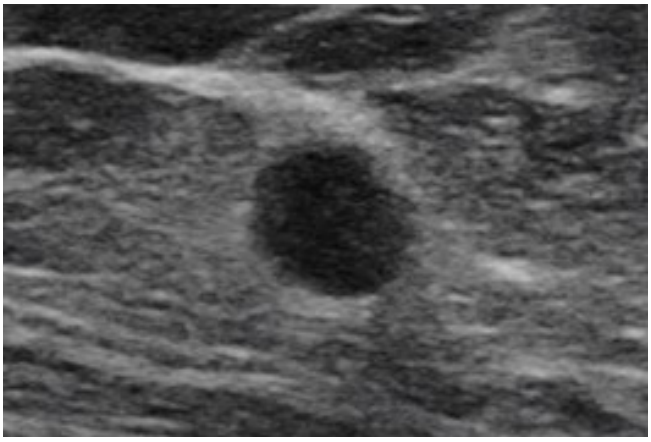

Fig. 1. Small, hypoechogenic TNBC with non-circumscribed margins and hyperechogenic halo

When analyzing the elastograms, in most cases, increased stiffness of TNBC was observed at the periphery of the lesion, whereas the central part of the tumors had either a heterogeneous stifness, were coded as soft or showed poor shear wave penetration. In the FA group, stiffer areas were more often located inside the lesion, whereas its periphery and surrounding tissues were soft.

Other publications present similar conclusions on the value of elastography, emphasizing that it significantly improves the sensitivity and specificity of ultrasonography[8,14,17–22].

In TNBC, increased stiffness is explained by the tumor's high cellularity and compression of surrounding tissues[23]. FAs and benign lesions rarely show E_{max} >160 kPa. A moderate increase in stiffness may occur in FA subtypes other than simple (complex, hypercellular, or complicated[24], in large lesions growing superficially, in a dense glandular tissue, or when hyalinization occurs[25,26].

In SG, echogenicity of the lesions also turned out to be an important parameter – 15/16 TNBCs (94%) were assessed as hypoechoic, and 63% of FAs were assessed as "other than hypoechoic". Hypoechogenicity is a feature of hypercellular lesions.

The presence of a hyperechoic halo also demonstrated good specificity. In the study group, this feature among FA lesions occurred with a low frequency (15.7% vs. 68% in the TNBC group). Internal vascularity was demonstrated in approximately 93% of TNBCs and 63% of FAs. This feature helps differentiate TNBCs from cysts, in which vascularity is not observed, but is less reliable in the differentiation from FAs.

Simultaneous analysis of multiple imaging parameters improves the ability to differentiate between TNBC and benign lesions. In TG, the best results were obtained for the following combinations: non-circumscribed margins and irregular shape; elastography other than soft and irregular shape; and non-circumscribed margins and the presence of vascularity in CD (AUC = 0.858; 0.836; 0.826). In SG, an AUC >0.9 was achieved for the following combinations: irregular shape and hypoechogenicity; non-circumscribed mar-

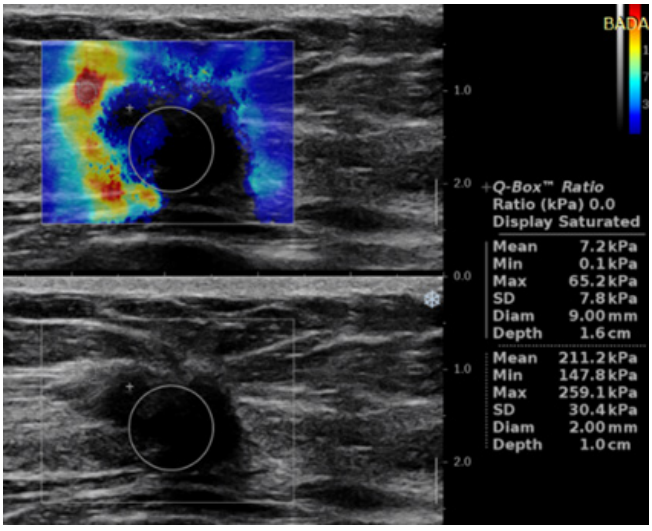

Fig. 2. TNBC showing high stiffness on the periphery of the tumor – E_{max} 259 kPa

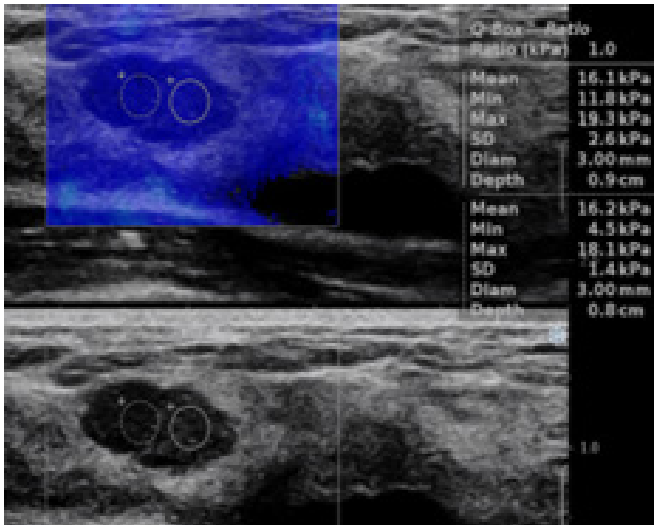

Fig. 3. Homogeneously soft FA – E_{max} 19 kPa

gins and hypoechogenicity; and non-circumscribed margins and irregular shape and hypoechogenicity. Combining three features also resulted in effective outcomes but not better than two-feature models.

The outcomes of the study differ from the observations presented in earlier works, where up to 41% of the lesions showed benign morphology[14,5,8,27,28]. When analyzing the methodologies of these studies, it is worth noting that most used transducers with a low upper-frequency band (up to 14–15 MHz), which affects image resolution and may have impaired the assessment of lesion margins. In the present study, a high-frequency transducer (18–5 MHz) was used along with sonoelastographic evaluation. In TG, no TNBC was classified as having circumscribed margins, the shape in 95% of the lesions was assessed as irregular, and only two lesions (5%) were considered oval. In SG, findings regarding shape and margins were similar. Adding information about stiffness further improved lesion differentiation.

The study was limited by the small number of tumors, particularly those <20 mm. Some tumors were assessed after biopsy, which may have influenced their presentation. Additionally, not all FAs were confirmed by biopsy.

Conclusions

Differentiation between TNBC and benign lesions in multiparametric ultrasonography using high-frequency transducers is effective. Additional assessment with SWE sonoelastography significantly improves diagnostic accuracy by providing insight into processes occurring on the periphery of proliferative lesions. Increased hardness around the tumor should prompt biopsy, as this phenomenon is rare in benign lesions.

B-mode features to be sought during the examination include irregular shape and non-circumscribed tumor margins. The presence of such features, even in a small part of the lesion, excludes it from the BI-RADS3 category. Hypoechogenicity, a hyperechogenic halo, and vascularity within the lesion are other parameters helpful in differentiation. Combined assessment of these features increases both the sensitivity and specificity of ultrasonography.

Conflict of interest

The authors do not report any financial or personal connections with other persons or organizations which might affect the contents of this publication and/or claim authorship rights to this publication.

Acknowledgements

The authors would like to thank the radiologists and pathologist at the Maria Skłodowska-Curie Memorial Cancer Center and Institute of Oncology, Warsaw, Poland, for their contribution to data collection.

Author contributions

Original concept of study: MG. Writing of manuscript: MG. Analysis and interpretation of data: MG, KDS. Final acceptation of manuscript: MG, KDS. Collection, recording and/or compilation of data: MG, KDS. Critical review of manuscript: MG, KDS.

References

1. Yoon GY, Cha JH, Kim HH, Shin HJ, Chae EY, Choi WJ: Sonographic features that can be used to differentiate between small triple-negative breast cancer and fibroadenoma. Ultrasonography 2018; 37: 149–156. doi: 10.14366/usg.17036.
2. Schopp JG, Polat DS, Arjmandi F, Hayes JC, Ahn RW, Sullivan K *et al.*: Imaging challenges in diagnosing triple-negative breast cancer. Radiographics 2023; 43: e230027. doi: 10.1148/rg.230027.
3. Howard FM, Olopade OI: Epidemiology of triple-negative breast cancer: a review. Cancer J 2021; 27: 8–16. doi: 10.1097/PPO.0000000000000500.
4. Li L, Zhong Y, Zhang H, Yu H, Huang Y, Li Z *et al.*: Association between oral contraceptive use as a risk factor and triple-negative breast cancer: A systematic review and meta-analysis. Mol Clin Oncol 2017; 7: 76–80. doi: 10.3892/mco.2017.1259.
5. Dogan BE, Turnbull LW: Imaging of triple-negative breast cancer. Ann Oncol 2012; 23 Suppl 6: vi23–29. doi: 10.1093/annonc/mds191.
6. Adrada BE, Moseley TW, Kapoor MM, Scoggins ME, Patel MM, Perez F *et al.*: Triple-negative breast cancer: histopathologic features, genomics, and treatment. Radiographics 2023; 43: e230034. doi: 10.1148/rg.230034.
7. Johnson KS, Conant EF, Soo MS: Molecular subtypes of breast cancer: a review for breast radiologists. J Breast Imaging 2021; 3: 12–24. doi: 10.1093/jbi/wbaa110.
8. Dogan BE, Gonzalez-Angulo AM, Gilcrease M, Dryden MJ, Yang WT: Multimodality imaging of triple receptor-negative tumors with mammography, ultrasound, and MRI. AJR Am J Roentgenol 2010; 194: 1160–1166. doi: 10.2214/AJR.09.2355.
9. Zhang L, Li J, Xiao Y, Cui H, Du G, Wang Y *et al.*: Identifying ultrasound and clinical features of breast cancer molecular subtypes by ensemble decision. Sci Rep 2015; 5: 11085. doi: 10.1038/srep11085.
10. Barr RG, Nakashima K, Amy D, Cosgrove D, Farrokh A, Schafer F *et al.*: WFUMB guidelines and recommendations for clinical use of ultrasound elastography: Part 2: breast. Ultrasound Med Biol 2015; 41: 1148–1160. doi: 10.1016/j.ultrasmedbio.2015.03.008.
11. Chen IE, Lee-Felker S: Triple-negative breast cancer: multimodality appearance. Curr Radiol Rep 2023; 11: 53–59. doi: 10.1007/s40134-022-00410-z.
12. Derakhshan F, Reis-Filho JS: Pathogenesis of triple-negative breast cancer. Annu Rev Pathol 2022; 17: 181–204. doi: 10.1146/annurev-pathol-042420-093238.
13. Li JW, Zhang K, Shi ZT, Zhang X, Xie J, Liu JY, Chang C: Triple-negative invasive breast carcinoma: the association between the sonographic appearances with clinicopathological feature. Sci Rep 2018; 8: 9040. doi: 10.1038/s41598-018-27222-6. Erratum in: Sci Rep 2020; 10: 4468. doi: 10.1038/s41598-020-61260-3.
14. Yeo SH, Kim GR, Lee SH, Moon WK: Comparison of ultrasound elastography and color doppler ultrasonography for distinguishing small triple-negative breast cancer from fibroadenoma. J Ultrasound Med 2018; 37: 2135–2146. doi: 10.1002/jum.14564.
15. Avdan Aslan A, Gültekin S, Karakoç E, Tosun SN: Impact of menopausal status on imaging findings of patients with triple-negative breast cancer. J Breast Imaging 2022; 4: 384–391. doi: 10.1093/jbi/wbac027.
16. Candelaria RP, Adrada BE, Wei W, Thompson AM, Santiago L, Lane DL *et al.*: Imaging features of triple-negative breast cancers according to androgen receptor status. Eur J Radiol 2019; 114: 167–174. doi: 10.1016/j.ejrad.2019.03.017.
17. Berg WA, Cosgrove DO, Doré CJ, Schäfer FK, Svensson WE, Hooley RJ *et al.*; BE1 Investigators: Shear-wave elastography improves the specificity of breast US: the BE1 multinational study of 939 masses. Radiology 2012; 262: 435–449. doi: 10.1148/radiol.11110640.
18. Wang F, Wang H: Diagnostic value of ultrasound elastography in triple negative breast cancer: A meta-analysis. Medicine (Baltimore). 2023; 102: e32879. doi: 10.1097/MD.0000000000032879.
19. Cho N, Jang M, Lyou CY, Park JS, Choi HY, Moon WK: Distinguishing benign from malignant masses at breast US: combined US elastography and color doppler US –influence on radiologist accuracy. Radiology 2012; 262: 80–90. doi: 10.1148/radiol.11110886.

20. Dobruch-Sobczak K, Gumowska M, Mączewska J, Kolasińska-Ćwikła A, Guzik P: Immunohistochemical subtypes of the breast cancer in the ultrasound and clinical aspect – literature review. J Ultrason 2022; 22: 93–99. doi: 10.15557/JoU.2022.0016.
21. Gumowska M, Mączewska J, Prostko P, Roszkowska-Purska K, Dobruch-Sobczak K: Is there a correlation between multiparametric assessment in ultrasound and intrinsic subtype of breast cancer? J Clin Med 2021; 10: 5394. doi: 10.3390/jcm10225394.
22. Biondić Špoljar I, Ivanac G, Radović N, Divjak E, Brkljačić B: Potential role of shear wave elastography features in medullary breast cancer differentiation. Med Hypotheses 2020; 144: 110021. doi: 10.1016/j.mehy.2020.110021.
23. Sheng C, Gao S, Yan L, Yin H, Hu J, Ye Z, Wei X: Application value of conventional ultrasound combined with shear wave elastography in diagnosing triple negative breast cancer. Gland Surg 2021; 10: 1980–1988. doi: 10.21037/gs-21-320.
24. Başara Akın I, Özgül H, Altay C, Seçil M, Durak MG, Gürel D, Balcı P: Use of shear-wave elastography to distinguish complex and complicated fibroadenomas from simple fibroadenomas. Diagn Interv Radiol 2023; 29: 674–681. doi: 10.4274/dir.2022.221615.
25. Elseedawy M, Whelehan P, Vinnicombe S, Thomson K, Evans A: Factors influencing the stiffness of fibroadenomas at shear wave elastography. Clin Radiol 2016; 71: 92–95. doi: 10.1016/j.crad.2015.10.029.
26. Basara Akin I, Ozgul HA, Guray Durak M, Balci P: Evaluation of elastographic features in complex fibroadenomas with radiologic-pathologic correlation. J Ultrasound Med 2021; 40: 1709–1718. doi: 10.1002/jum.15534.
27. Ko ES, Lee BH, Kim HA, Noh WC, Kim MS, Lee SA: Triple-negative breast cancer: correlation between imaging and pathological findings. Eur Radiol 2010; 20: 1111–1117. doi: 10.1007/s00330-009-1656-3.
28. Candelaria RP, Spak DA, Rauch GM, Huo L, Bassett RL, Santiago L *et al.*: BI-RADS ultrasound lexicon descriptors and stromal tumor-infiltrating lymphocytes in triple-negative breast cancer. Acad Radiol 2022; 29 (Suppl 1): S35–S41. doi: 10.1016/j.acra.2021.06.007.